Journal of Arid Environments 84 (2012) 38–50

Contents lists available at SciVerse ScienceDirect

Journal of Arid Environments

journal homepage: www.elsevier.com/locate/jaridenv

Analysis of vegetation seasonality in Sahelian environments using MODIS LAI, in association with land cover and rainfall

C. Bobée [a,*], C. Ottlé [a], F. Maignan [a], N. de Noblet-Ducoudré [a], P. Maugis [a], A.-M. Lézine [a], M. Ndiaye [b]

[a] Laboratoire des Sciences du Climat et de l'Environnement, LSCE-IPSL (CEA-CNRS-UVSQ), Ormes des merisiers, 91191 Gif-sur-Yvette Cedex, France
[b] Agence Nationale de la Météorologie du Sénégal, Aéroport Léopold Sédar SENGHOR, BP 8257 Dakar Yoff, Senegal

ARTICLE INFO

Article history:
Received 23 May 2011
Received in revised form
13 February 2012
Accepted 9 March 2012
Available online xxx

Keywords:
Land cover
MODIS LAI product
Rainfall
Vegetation phenology

ABSTRACT

Present-day Sahelian vegetation in a highly anthropized semi-arid region is assessed from local to regional scales, through the joint analysis of MODIS LAI (1 km^2 and 8-day resolutions), daily rainfall, morphopedological and land cover datasets covering the period 2000–2008. The study area is located in northwest Senegal and consists of the "Niayes" and the northwestern "Peanut Basin" eco-regions, characterized by market gardening and rain-fed cultivated crops, respectively. The objectives are i) to analyse at pixel scale LAI time series and their relation to vegetation and soil types, ii) the estimation of phenological metrics (start of season SOS, end of season EOS, growing season length GSL) and their inter-annual variability, iii) to recognize the vegetation responses to rainfall trends (mean annual precipitation, MAP; frequency of rainy events, K; combination of MAP and K, called F).

Pixel-scale analyses show that LAI time series 1) describe the actual phenology (agreeing with ground-truth AGHRYMET data), and thus can be used as a proxy for Sahelian vegetation dynamics, 2) are strongly dependent on soil types. Median maps of SOS and EOS suggest an increase of the GSL from Saint-Louis to Dakar, in agreement with both the North-South rainfall gradient and the intensification of agricultural practices around Dakar. Significant correlations (*R*: 0.64) between annual variation coefficient of LAI and MAP for both herbaceous crops and natural vegetation are highlighted; this correlation is reinforced (*R*: 0.7) using the rainfall distribution factors *K* and *F*. Rainfall thresholds allowing the SOS can be defined for each type of vegetation. These thresholds are estimated at 0–5 mm, 20 mm and 40 mm for natural herbs, herbaceous crops and shrublands, respectively.

If previous works revealed the close link between the MAP and the SOS, our results highlight that LAI dynamics are also controlled by rainfall distribution during the Monsoon season. In this study, climatic indicators are proposed for estimating vegetation dynamics and monitoring SOS. Coupling Earth Observation data, such as MODIS LAI, with rainfall data, vegetation and soil information is found to be a reliable method for vegetation monitoring and for assessing the impact of human pressure on vegetation degradation.

1. Introduction

The Sahel has experienced a rainfall decline over the last decades (Gonzalez, 2001; Nicholson, 2000). Although a recent shift to a wetter regime has been observed (Nicholson, 2005; Olsson et al., 2005), except for western Sahel (Lebel and Ali, 2009), the major droughts (1972–1973 and 1983–1984 events) that occurred within the 1968–1993 dry period led to a decrease in water resources, to the land cover degradation, and had severe impacts on crop productivity and populations (Tschakert, 2007).

The determination of the predominant factor responsible for land degradation is still questionable. Gonzalez (1997) suggested the predominance of climatic factors when Tappan et al. (2000, 2004) put the emphasis on traditional land-use practices, such as crop expansion in association with an intensification of deforestation. However, for the UNCCD (United Nations, 1994), the observed Sahelian vegetation results from a complex combination of both anthropogenically induced degradation effects and climatic trends. From local to regional scales, parameters such as soil types, vegetation communities, inter-annual variations in rain-use efficiency are also responsible for biomass productivity variations (Diouf and Lambin, 2001; Hiernaux et al., 2009; Tottrup and Rasmussen, 2004).

* Corresponding author. Tel.: +33 6 30 28 01 04.
E-mail address: cecilia.bobee@gmail.com (C. Bobée).

0140-1963/$ – see front matter © 2012 Elsevier Ltd. All rights reserved.
doi:10.1016/j.jaridenv.2012.03.005

Assessing land cover changes is one of the bases for modelling vegetation seasonality in response to climatic changes. One means of assessing the seasonality of Earth's vegetated surfaces is to use remotely sensed data (Tucker et al., 1985). Among the array of available Earth Observation products, the *Leaf Area Index* (LAI) product provided by the MODerate resolution Imaging Spectroradiometer (MODIS) proved to be a significant biophysical parameter for crop yield assessment (Doraiswamy et al., 2005). This product is obtained from solar reflectances by radiative transfer model inversions, and is defined as one-sided green leaf area per unit ground area (Myneni et al., 1997). Among the few studies validating the MODIS LAI product in semi-arid environments, good correlations between *in situ* LAI measurements and MODIS LAI in the Southern Kalahari (Privette et al., 2002) and in Central and North Senegal (Fensholt et al., 2004) have been reported. At the African continent scale, the LAI product was used for discriminating vegetation types and proved to contain major information for characterizing plant phenological properties, i.e. the timing and the dynamics of the vegetation-growing season (Kaptue et al., 2010): the LAI spatial pattern indeed matches the vegetation cover distribution and the LAI time series follows the intra-annual dynamics of vegetation cycle, conditioned by local environmental conditions such as rainfall or topography. For Fensholt et al. (2004), MODIS LAI product retranscribes the "real-world LAI" and thus may be used as a vegetation status proxy.

In the last decades, an array of methods has been developed for determining the timing of the growing season (Kang et al., 2003; Schwartz, 1998; White et al., 2002; Zhang et al., 2003) from remotely sensed time series. The vegetation dynamics may be defined by the identification of phenological key dates, usually the green-up (Start Of the growing Season, SOS), the maturity, the senescence (End Of the growing Season, EOS) and the Growing Season Length (GSL). In semi-arid regions, vegetation phenology is mainly controlled by water availability (Kramer et al., 2000). Green leaves indeed often follow rainfall events (De Bie et al., 1998; Peñuelas et al., 2004). In cropland areas, growth and harvest dates were also revealed to be controlled by the distribution and amounts of precipitation during the rainy season (Omotosho, 1992), as well as the number and frequency of dry-days within the monsoon season (Proud and Rasmussen, 2011). A quantitative understanding of the relation between climatic trends and growing season seasonality may improve the ability to predict food production and anticipate biomass reduction (Brown and de Beurs, 2008).

The aim of this study is to assess vegetation dynamics under anthropized semi-arid environments through the joint analysis of MODIS LAI, rainfall, geomorphological and land cover datasets over the period 2000–2008 (Fig. 2). The study area is located in Northwest Senegal and consists of the "Niayes" and the north-western "Peanut Basin" Eco-regions (Tappan et al., 2004). This region was chosen to analyse the links between vegetation seasonality, soil characteristics and rainfall for two main reasons. First, this area constitutes a representative case of degraded Sahelian vegetation (Tappan et al., 2004). Second, daily rainfall data provided by the "Direction Nationale de la Météorologie" (DNM, Dakar) was available at four rain gauge stations. This dataset permitted us to analyse the spatial and temporal vegetation responses to rainfall.

The main objectives reported in this paper are as follows (Fig. 2):

- Study of the vegetation seasonality from LAI time series.
- Estimate of phenological metrics, their spatial variations and their inter-annual variability.
- Analysis of the vegetation responses to rainfall amount and distribution.

The first objective concerns the detailed analysis of LAI time series, and is performed at local scale. Cross-correlations between LAI time series, types of vegetation (including *in situ* agricultural information) and rainfall patterns are discussed for selected LAI pixels.

The second objective aims at deriving phenological information from LAI time series at regional scale. The derivation of SOS and EOS dates, as well as GSL, is performed using the methodological approach proposed by Zhang et al. (2003), which consists of fitting two simple sigmoid function to remote sensing time series to extract the phenological information.

Finally, the third objective relies on the assessment of the influence of rainfall patterns (annual amount of rain and frequency of rainy events) on the timing and the performance of the vegetation types encountered in the study area. These correlations are analysed only around the four rain gauge stations, with a particular focus on the assessment and characterization of the rainfall-phenology relationships according to vegetation and soil types.

2. Study area

2.1. Geographical setting

The study area is located in northwest Senegal, in a 40 km wide strip of land along the Senegal coastland, stretching over 180 km between the cities of Dakar and Saint-Louis (Fig. 1). The topography presents live sand dunes ranging between 0 and 50 m above sea level and reaching an altitude of 126 m near the plateau of Thiès. The study area covers two eco-regions characterized by differences in geomorphological setting (Stancioff et al., 1986), floral composition and land use practices (Tappan et al., 2004). The Long Coast eco-region defines a narrow 5–30 km wide land strip along the northern Senegalese coastline, and consists of a succession of sandy dunes and organic-hydromorphic soils, also referred to as peat soils, in depressions (Tappan et al., 2004). The north-western part, the "Peanut Basin" eco-region is composed of eolian sands on which have developed ferruginous tropical sandy soils, the latter being brown, deep, structureless and well-drained (Tschakert and Tappan, 2004). Southwards, ferruginous tropical soils are developed on marno-calcareous formations (near Thiès, Fig. 1).

2.2. Vegetation

Global information on vegetation spatial distribution for the two studied eco-regions is shown in Fig. 1 (source Globcover Land Cover -GLC- map, see the description of the product in section 3.3). The Long Coast eco-region is characterized by the presence of niayes, which are microecosystems in inter-dunal depressions, and Savanna shrub in surrounding sandy dunes. The location of the niayes is reported in Fig. 1 (from the Global Land Cover Network -GLCN- database, http://www.glcn.org/dat_0_en.jsp website). Since the beginning of the 1970s, the natural vegetation of the niayes has progressively been replaced by market gardening (Tappan et al., 2004). Representing less than 1% of the study area, the vegetation dynamics of these particular irrigated environments are not discussed in the study.

Vegetation in the Peanut Basin essentially consists of a patchwork of crops and sparse shrublands. Rainfed millet (85–90 day growth cycle) and peanut (90–105 day growth cycle) systems are used in yearly rotation (Affholder, 1995).

3. Datasets

3.1. Precipitation data

Daily rainfall data was provided by the "Direction Nationale de la Météorologie" (DNM, Dakar, Senegal). Four rain gauge stations

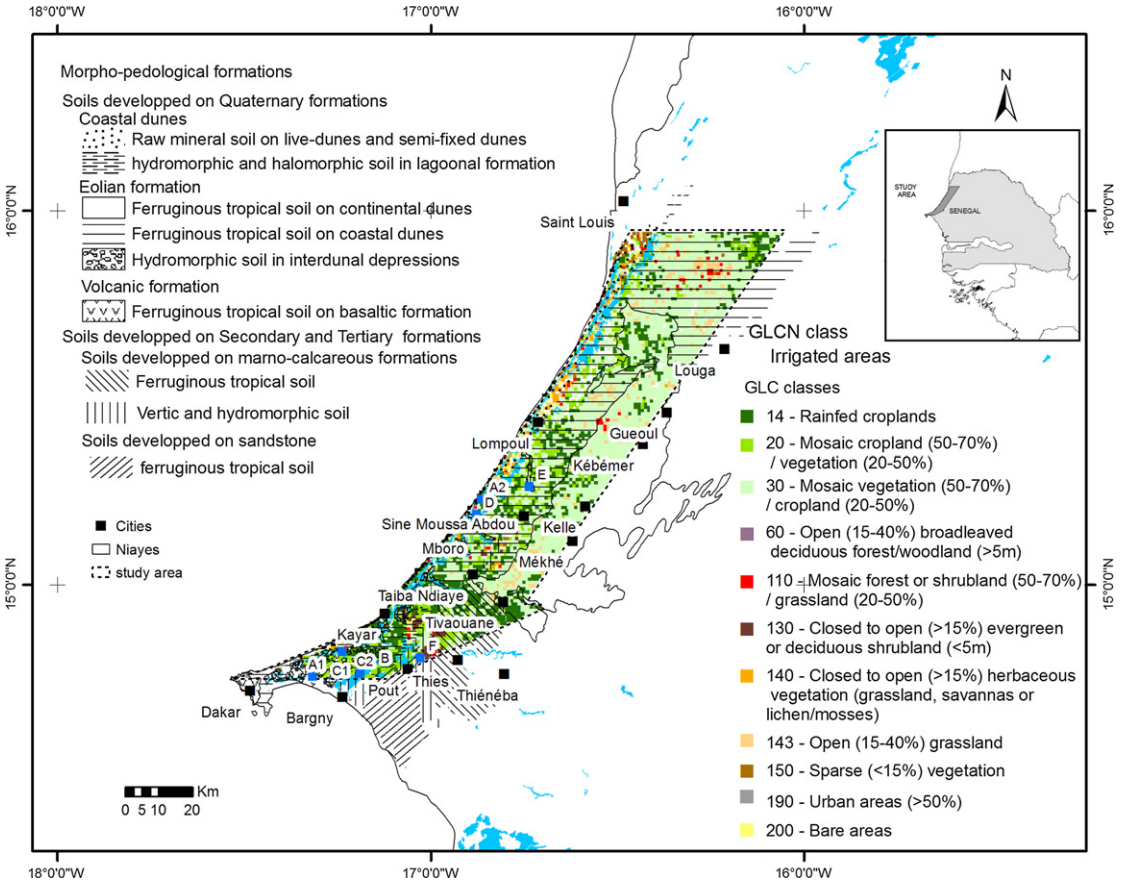

Fig. 1. Vegetation land cover map (GLC legend) aggregated to 1 km^2 resolution (WGS-84 coordinate system). The Morpho-pedological setting (from Stancioff et al., 1986, modified map) and the location of irrigated areas (GLCN legend) are superimposed to the land cover map. Blue dots (Labelled A1 to F) correspond to the location of extracted LAI pixels.

distributed across the studied region were available for the period 2000–2008. They are located at Thiès, Louga, Saint-Louis and Dakar (Fig. 1, Table 1). It should be noticed that the rainfall dataset for 2004 is not complete for the Thiès rain gauge station and was not considered in this study. The study area is characterized by high extra-seasonal and inter-annual rainfall mainly concentrated in the core of the monsoon season, which lasts from June to October (Table 1). Several minor rainy events, referred to as "Heug rains" (Le Borgne, 1979), occurring during winter and linked to polar air intrusions, were observed during the period 2000–2008. Mean annual precipitation (MAP) for the period 2000–2008 equals 282.5 ± 60.0 mm (mean $\pm$ standard deviation) and 296.2 ± 150.6 mm at the rain gauge stations of Saint-Louis and Dakar, respectively (Table 1). The spatial distribution of rainfall in this zone follows the latitudinal gradient, but is also influenced by topography, with a cumulative rainfall of 511.1 ± 212.1 mm recorded at the plateau of Thiès (Table 1).

3.2. MODIS LAI products

The MOD15A2 LAI product used in this work is based on the MODIS TERRA sensor (Collection 4). This 8-day composite product is provided at a 1 km^2 spatial resolution. MODIS LAI data, originally projected onto an integerized sinusoidal grid, was extracted and reprojected onto the WGS-84 coordinate system, and reported in a Geographic Information System (ArcGIS 9.2, ESRI Corp, Redlands, CA, USA). The theoretical basis of the MODIS LAI product algorithm, implementation aspects and validation results are detailed in Knyazikhin et al. (1999) and Myneni et al. (2002). The LAI product is based on biome-specific algorithms, involving several constants

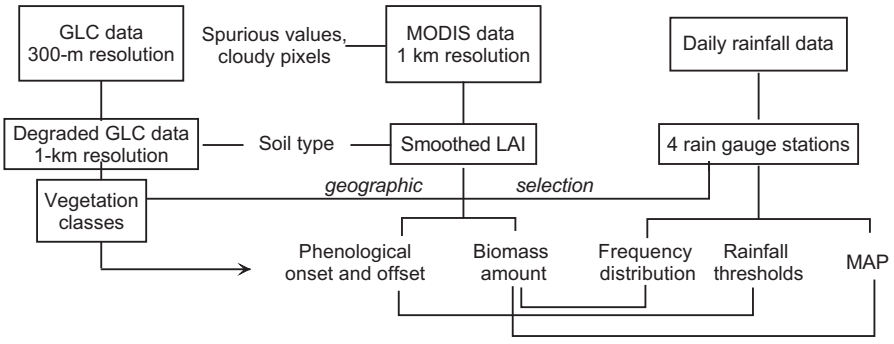

Fig. 2. Methodological approach for correlating GLC, soil types, MODIS and rainfall datasets.

Table 1
Rainfall distribution during the Monsoon season for the period 2000–2008 (MAP: mean annual precipitation (mm); RD: number of rainy events; BR: beginning of the rainy season (DOY); ER: end of the rainy season (DOY); RS: duration of the rainy season; (s: standard deviation).

		2000	2001	2002	2003	2004	2005	2006	2007	2008	Mean $\pm 1\sigma$
Dakar	MAP	202.5	232.2	113.5	208.9	281.8	485.9	281.9	263.0	596.2	296.2 ± 150.6
	RD	33	32	16	20	23	32	25	21	39	26.8 ± 7.5
	BR	173	185	157	192	155	179	166	165	184	172.9 ± 13.0
	ER	291	307	282	295	280	318	285	271	297	291.8 ± 14.4
	RS	118	122	125	103	125	139	119	106	113	118.9 ± 10.9
Thies	MAP	607.9	594.2	390.6	404.0	–	556.7	317.9	578.0	639.7	511.1 ± 212.1
	RD	45	34	28	39	–	29	33	30	45	35.4 ± 6.9
	BR	187	182	169	158	–	178	165	206	164	176 ± 15.6
	ER	292	284	291	294	–	282	287	286	293	288.6 ± 4.5
	RS	105	102	122	136	–	104	122	80	129	112.5 ± 18.1
Louga	MAP	374.6	261.4	196.3	153.2	372.9	361.1	272.6	227.3	374.6	288.2 ± 58.7
	RD	33	27	17	31	23	36	25	19	29	26.7 ± 6.3
	BR	179	185	168	179	193	166	165	191	179	178.3 ± 10.4
	ER	268	274	284	294	271	299	287	281	268	280.7 ± 11.3
	RS	89	89	116	115	78	133	122	90	89	102.3 ± 19.2
Saint-Louis	MAP	332.5	275.7	282.5	351	139	281.2	294.6	310.7	275	282.5 ± 60.0
	RD	25	32	25	31	24	37	28	22	39	29.2 ± 6.0
	BR	188	185	168	192	205	167	177	210	191	187.0 ± 14.8
	ER	291	274	284	295	270	318	287	273	277	285.4 ± 14.9
	RS	103	89	116	103	65	151	110	63	86	98.4 ± 27.1

(leaf angle distribution, optical properties of soils and wood, and canopy heterogeneity), and obtained by inversion of the 3-dimensional radiative transfer model (Myneni et al., 1997). This product may be corrupted by clouds or atmospheric effects (Myneni et al., 2002) and, in this case, a back-up algorithm based on the empirical relationship between FPAR/LAI (FPAR being the Fraction of Photosynthetically Active Radiation (400–700 nm) absorbed by vegetation) and NDVI (Normalized Difference Vegetation Index) is applied. In Sahelian environments, Fensholt et al. (2004) reported that the MODIS LAI products correlate strongly with *in situ* LAI measurements.

3.3. Land cover data

The regional (African continent) Globcover Land Cover (GLC) map (Bicheron et al., 2006) was used to characterize land cover at the MODIS pixel scale. The GLC product has a 300m spatial resolution covering the period December 2004–June 2006. It was derived by processing full resolution images from the European MERIS/ENVISAT sensor. A total of 11 land cover classes, referring to the Land Cover Classification System (LCCS), have been defined over the study area. The GLC nomenclature is detailed in Fig. 1. The main classes are essentially rain-fed croplands (type GLC14), in most cases in association with a mosaic of grasslands, shrublands and forests (GLC20 and GLC30 classes). Closed to open natural herbaceous vegetation (GLC140 and GLC143 classes), in association with a patchwork of forest shrubland/grassland (GLC110 class) is mainly concentrated in the Long Coast eco-region, but also occurs between the cities of Saint-Louis and Tivaouane as scattered-isolated vegetation. Sparse vegetation (GLC150 class) is also observed near the cities of Dakar and Saint-Louis. The natural vegetation is predominantly composed of open broadleaved deciduous forest/woodland (GLC60 class) and closed to open shrublands (GLC130 class) between the cities of Kayar and Thiès. The intensification of agricultural practices is revealed by the predominance of GLC14 and GLC20 classes (Fig. 1) both south and north from this transect, while patchworks with less cropland (GLC30) are dominant in the northern part of the study area (north of Tivaouane). In the Long Coast eco-region, the bare soil areas (GLC200 class), or live-dune systems, are characterized by the presence of rain-fed evergreen tree plantations (Casuarina equisetifolia J.R. & G. Forst). This drought-tolerant whispering pine tree was established in the eighties, for the stabilization of sand dunes and the preservation of niaye depressions (the GLCN class, Fig. 1).

We used additional agricultural *in situ* information, provided by the AGHRYMET Centre (downloadable at http://www.agrhymet.ne). Analysis was performed for the Year 2006, year for which a complete series of 10-daily bulletins accurately describing the crop phenology in the Thiès region, is available.

4. Methodological approach

4.1. LAI filtering

The MODIS-LAI time series present spurious values and greater noise during the monsoon season. These problems are largely caused by errors in the cloud masking process, or sometimes also by instrument deficiencies. In order to filter out false data, a five-point moving average was applied on the MODIS-LAI time series for entire annual cycles (Jiang et al., 2010).

4.2. Phenological analysis

4.2.1. Determination of SOS, EOS and GSL

Several methodologies have been suggested to determine the timing of the vegetation phenology (SOS and EOS) from remotely sensed data. These methods have employed numerous approaches, for example using mid-point value (White et al., 1997) or empirical equations (Zhang et al., 2003). In this work, we have used two logistic functions for fitting the LAI time series and extracting the SOS and EOS dates.

The phenological analysis was performed between DOY (day of year) 57 (26 February) in 2000 and DOY 361 (27 December) in 2008. The estimation of the phenological metrics follows a two step approach. First, the MODIS LAI values were fitted to two sigmoidal functions for the greenness and senescence periods. Such an approach has been proposed by several authors, either by modelling separately the greenness and senescence periods using two different sigmoidal functions (Zhang et al., 2003) or by simulating the whole phenological cycle using one double sigmoidal function

(Fisher and Mustard, 2007). The approach proposed by Zhang et al. (2003) is applied in the current analysis for fitting LAI time series. It is based on the fitting of a 4-parameter sigmoidal function. The choice of using two simple sigmoidal functions (instead of a double-sigmoid function) results in the greater enhancement of the senescence period fitting. The modelling of the greenness period, using an open window on the period DOY 153-281, is defined as follows:

$$A(t) = A_1 + A_2\left(\frac{1}{1+e^{m-nt}}\right) \quad (1)$$

where $A(t)$ is the fitted LAI signal during the greenness period at DOY t, A_1 is the background LAI, A_2 is the total amplitude of the LAI signal and, m and n are fitting parameters. In the same way, the senescence period was fitted by a second sigmoid function, defined as the inverse of Eq. (1). The time period chosen to adjust the senescence curve is DOY 233-361. An example of the greenness and senescence fits is given in Fig. 3. We used two different temporal windows for modelling the greenness and the senescence periods independently. Phenology modelling focuses on the DOY 150-361 period in order to avoid the modelling of the early greenness peaks in irrigated areas or linked to the Heug rainy events (occurring both in winter). So, Considering only the time window DOY 150-361, this phenological study focuses on rain-fed vegetation. Pixels for which standard deviations between growth and senescence sigmoid fits and LAI data exceed 5% were removed from the modelled dataset, which not exceed 7% of the annual LAI databases. Here, SOS and EOS are defined respectively as the dates for which the greenness and senescence sigmoids equal 10% of their amplitude. These dates have been estimated, pixel by pixel, and their difference allows us to calculate the GSL. Maps of SOS, EOS and GSL were extracted for each year between 2000 and 2008 on the whole study area at the MODIS pixel scale.

4.2.2. Estimation of vegetation dynamics

The dynamics of the annual phenological cycle are referred in this study as the amplitude of the annual LAI variations. In order to analyse the variations of vegetation dynamics, it has been found more robust to analyse the coefficient of variation (CV) of the LAI time series, instead of the unique LAI maximum value. By definition, this statistical parameter is the ratio of the standard deviation to the mean. It gives information about the relative spread in the

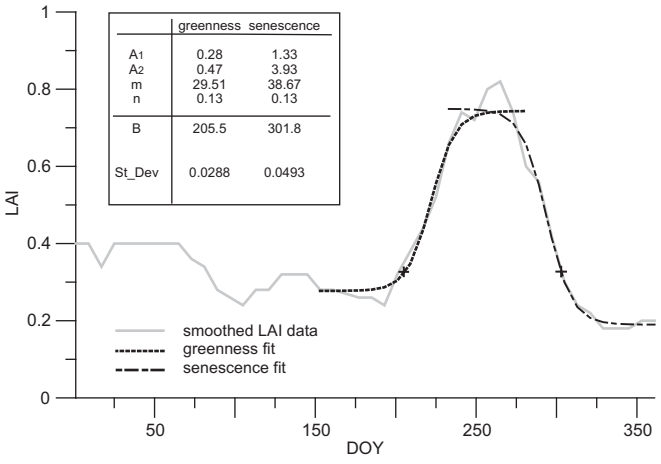

Fig. 3. Example of fit of greenness and senescence sigmoids (dashed curves) to one smoothed LAI profile (latitude: −16.310, longitude: 15.662, year: 2001). Fitting parameters and key phenological dates are reported in associated table. SOS and EOS correspond to 10% of the vegetation biomass for both growth and senescence periods, respectively. Axes are day of year (DOY) against LAI.

LAI dataset and allows the different vegetation dynamics to be compared. In this work, we provide and discuss a map of the temporal median value of the annual CV of LAI (MCV_LAI) for the 2000–2008 period.

4.3. Analysis of the links between soil type, rainfall and phenological parameters

According to previous works performed in the Sahel, rainfall is highly variable both spatially and temporally (Cuenca et al., 1997; Gaze et al., 1998). In the studied area, the MAP is driven by the African Monsoon, which follows a latitudinal gradient (positive from north to south), and by topography (proximity of the Thiès plateau). The complexity of sahelian precipitation systems does not allow us to apply simple interpolation functions for spatializing rainfall from rain gauge measurements. Therefore, the correlations between LAI and daily rainfall datasets have been analysed around the four synoptic rain gauge stations, where the precipitation may be assumed homogeneous. The merging process to compare the surface and rainfall fields follows a three-step approach (Fig. 2). First, a correlation was made between the Land Cover map and MODIS images in order to attribute a GLC vegetation code to each LAI pixel and derived phenological dates (SOS and EOS). LAI and GLC datasets having different spatial resolutions (1 km and 300 m, respectively), each LAI pixel was given the vegetation code using a majority rule algorithm inside a 1 km^2 grid. The resulting land cover map is thus brought down to a 1 km^2 resolution (Fig. 1), but still reflects the spatial distribution of the GLC vegetation. Secondly, this GLC-LAI dataset was extracted for each year within a 10 km radius area around the rain gauge stations of Thiès and Louga, and within 20 and 25 km radius from the rain gauge stations of Saint-Louis and Dakar, respectively. These different surface sizes have been defined as the maximal area around the meteorological station (with a 25 km radius limit) excluding urban areas and considering the spatial variability of Sahelian rain fields (Ali et al., 2003).

Relationships between environmental, climatic and phenological parameters are discussed at local and regional scales:

- Relationships between LAI signals and *in situ* crop phenology are discussed near the rain gauge station of Thiès, a region for which the phenology is particularly well documented for the year 2006 (AGHRYMET data).
- We analyse the links between LAI time series and soil types, first near the station of Dakar, second at regional scale (using the MCV_LAI, a meaningful statistical indicator of vegetation dynamics, previously defined in Section 4.2). Correlations between LAI signals and soil types should be interpreted carefully, owing to the occurrence of a large range of soil reflectance values, particularly in semi-arid regions. However, no particular offset among the different LAI series were observed during winter (all LAI cycles ranged between 0.2 and 0.3 $m^2\,m^{-2}$ at the beginning of the year 2005 for example, whatever the soil type), which suggests that the residual soil reflectance effects are not significant on MODIS LAI products, in this region.
- Relationships between LAI time series (and derived phenological indicators) and rainfall features are examined around the rain gauge stations. Four rainfall indicators are defined in this work. The MAP is well-known to be linked to annual biomass amounts (Diouf and Lambin, 2001) but it is not sufficient to explain the main characteristics of vegetation dynamics. So, we propose in this study to introduce a new parameter, K, defined as the ratio between the number of rainy events (RD) and the duration of the rainy season (RS, see

Table 1). The parameter K takes into account the annual frequency of rainfall events during the rainy season. Since the vegetation growth is both constrained by the temporal repartition of rainfall events and annual cumulative rainfall, a second parameter, F, defined as the product of MAP by K is proposed for the comparison with the derived phenology metrics. The correlations between the MAP, K and F parameters and MCV_LAI are analysed according to GLC vegetation types. Correlations between cumulative rainfall thresholds around the rain gauge stations and SOS dates are also examined.

Before showing the results, it has to be noticed that the choice of working at the LAI MODIS pixel scale conducts to uncertainties on correlations made with vegetation and soil types. Indeed, we had to spatially degrade the land cover information to a resolution of 1 km^2 using a majority vote algorithm. Moreover, the GLC classes used are themselves defined by ranges of mixed vegetation, leading to uncertainties on floristic composition. Furthermore, it is well-known that phenology seasonality is also controlled by local drainage conditions (topography, organic matter content, …) (Malhado et al., 2009). The latter factor is not considered in this study in reason of a lack of data and also because of the chosen 1 km^2 spatial resolution. So those lead to inherent biases on results and reproducible studies must be analysed with care.

5. Results and discussion

5.1. Characterization of the regional vegetation seasonality

In this section we show and discuss the relationships between MCV_LAI, considered as a proxy of vegetation biomass status, and rainfall, vegetation classes and soil types. This analysis is performed at the MODIS-LAI pixel scale, firstly at selected sites (see Fig. 1) for the characterization of LAI signatures according to vegetation type, and secondly, near the rain gauge stations of Thiès and Dakar for analysing the influences of rainfall patterns and soil types on the resulting LAI signals.

5.1.1. Temporal LAI variations

The main types of vegetation encountered in the study area consist of a patchwork of agricultural vegetation (forest plantations, orchards and herbaceous crops) and natural vegetation (essentially grasslands and shrublands). Temporal averages and standard deviations of smoothed LAI data for the period 2001–2008 are reported in Fig. 4(a–f) (the incomplete MODIS LAI dataset for the year 2000 was not considered). Plots correspond to the selected pixels shown in Fig. 1 (sites labelled A1 to F), each one being characterized by a single and homogeneous GLC vegetation type. It should be noted that all LAI time series exhibit a non-zero minimum LAI during winter, probably due to the presence of evergreen species (Fig. 4a, site A2 in Fig. 1). Irrigated crops (Fig. 4c, site C2 in Fig. 1) are characterized by bi-modal growing cycles occurring during winter and summer. All other vegetation types produce a unimodal growing cycle occurring during the Monsoon period and, in any case, the LAI maxima do not exceed a value of 2 $m^2 m^{-2}$. The first obvious feature is that, except for irrigated crops, none of these plots (Fig. 4a–f) provides a particular signature that could help us to characterize or distinguish natural from anthropogenic vegetations, or to derive useful information about land cover changes. For example, the averaged greenness seasonality for rain-fed herbaceous crops (Fig. 4c, site C1 in Fig. 1) and natural herbs (Fig. 4e, site E in Fig. 1) are very similar. In the same way, high inter-annual variability in LAI plots is observed at the beginning of the greenness period for both tree crops (Fig. 4b, site B in Fig. 1) and open shrubs (Fig. 4f, site F in Fig. 1), and does not allow us to distinguish the two types of vegetation. The low and flat LAI signals characterizing evergreen forests (Fig. 4a, site A2 in Fig. 1) and open trees natural vegetation (Fig. 4d, site D in Fig. 1) are also analogous. This result was not expected but could be explained by the patchy character of the sahelian landscapes, mixing various vegetations and the necessary heterogeneity at 1km scale, but also, by the intrinsic features of the MODIS LAI dataset. Indeed, this 8-day composite product, with the addition of the cloud filtering, is probably too smoothed to permit the differentiation of the respective phenology within pixel dominant vegetation. Therefore, the punctual analysis of MODIS LAI time series is not sufficient step for identifying vegetation dynamics.

5.1.2. Relationships between annual LAI signals, cropland phenology and rainfall

An additional study was performed at a local scale for analysing to what extent LAI signatures and phenological timings are controlled by rainfall temporal variations. This analysis was carried out around the rain-gauge station of Thiès in 2006 to take advantage of the *in situ* information provided by the AGHRYMET centre (downloadable at http://www.agrhymet.ne). The chosen LAI pixels belong to the GLC14 class, which is the main land cover class in a 10km radius area around the Thiès station. Spatial averages and standard deviations of the selected LAI data are plotted in Fig. 4g, as well as cumulative rainfall (station of Thiès) and AGHRYMET information (four phenological stages reported, referred as P1 to P4).

In 2006, the rain front moved northwards during the second ten-day period of June in north Senegal and reached the area of Thiès on DOY 165 (June, 14th, Table 1). According to AGHRYMET observations, three sowings under wet conditions were performed in central Senegal in the second half of June (DOY 165-184; June, 14th, 22nd and July, 3rd; period P1). However, only 1.1mm of rain was recorded over the region of Thiès between DOY 166 and DOY 196, which did not allow the emergence of crops. It is only during the second ten-day period of July (DOY 192-202, period P2) that stages of emergence/seedling to knottiness for groundnut were observed. The end of P2 coincides with the LAI onset as estimated from MODIS LAI product, and starts when cumulative rainfall reaches about 32mm. Between DOY 222 and DOY 232 (period S3), the status of crops was flowering for late groundnut and early millet, and ear emergence for early sorghum. During P3, the LAI signal increases from 51 $\pm$6% to 84 $\pm$ 2% of its maximum LAI signal value. Between DOY 233 and DOY 243 (period P4), pod formation for groundnut and flowering/ear emergence for millet were observed. At the end of P4, the maximum LAI signal was reached. In September, most crops were mature or harvested. Early millet was at maturity stage and early sorghum was at ear emergence stage when sorghum and late millet were at the heading/flowering stage. Phenological stages for groundnut ranged from flowering to harvesting. The decrease of LAI signal corresponding to the beginning of senescence starts at DOY 256 (September, 13th) and is in accordance with green crop observed for early groundnut. Whereas a greenness delay of a few weeks exists between early and late crops, the LAI seasonality fits very well with the *in situ* agricultural observations.

At 1 km^2 resolution, LAI time series coupled with *in situ* agricultural observations (AGHRYMET information), such as sowings and green leaf emergence to harvesting stages, correctly express the vegetation seasonality and prove to be helpful for agricultural vegetation monitoring.

5.1.3. Relationships between pluri-annual LAI signals, soil types and rainfall

The inter-annual LAI signals have been compared for the different vegetation classes and soil types available around the

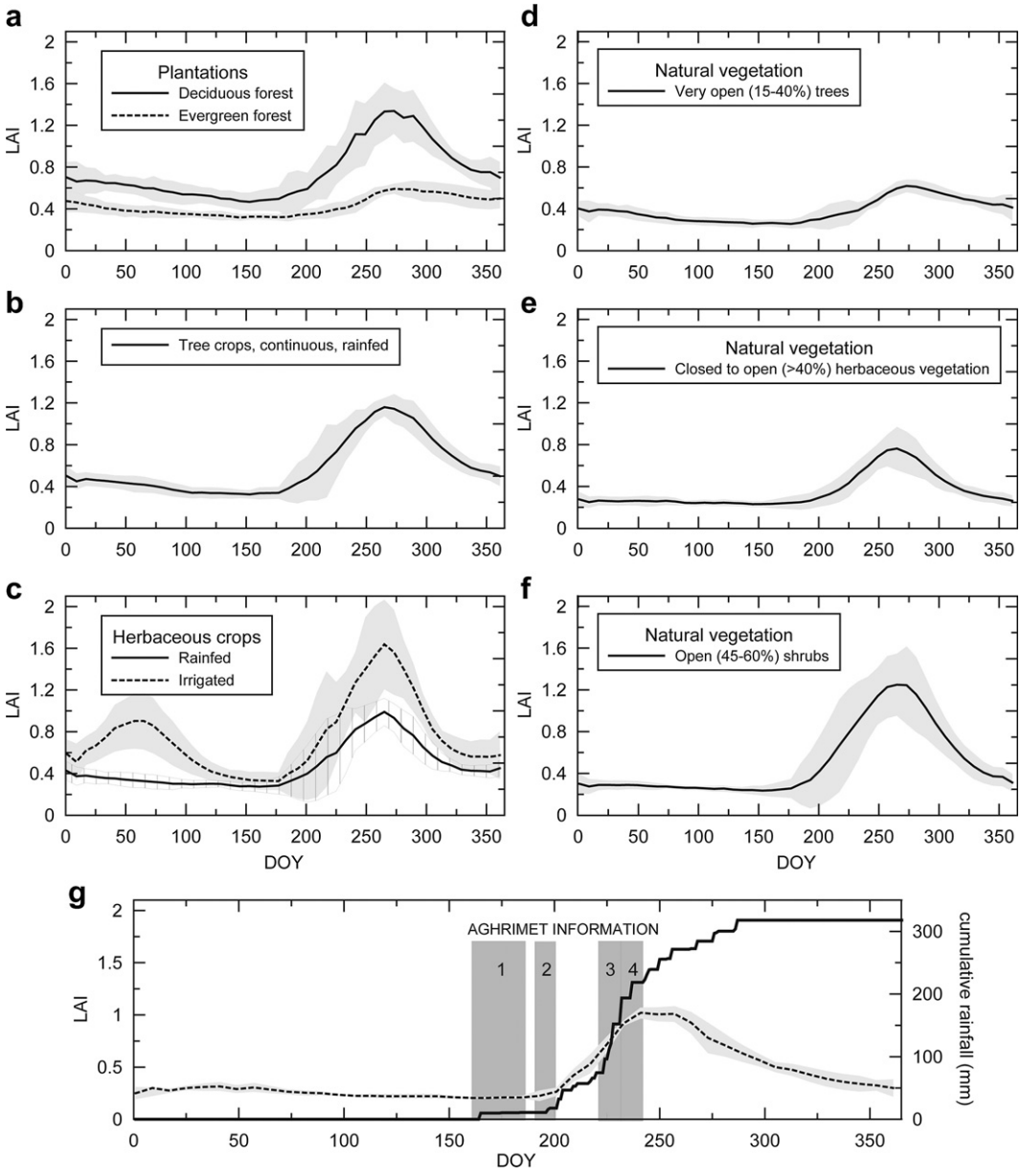

Fig. 4. (a–f) smoothed LAI averages (black lines) for the period 2001–2008 and representation of standard deviations (grey or hatched areas) for different types of vegetation. (g): Comparison between smoothed LAI average for rain-fed croplands (dashed curve) around Thiès and cumulative rainfall. (g) Agricultural stages (P1 to P4) observed (AGHRIMET information) for the year 2006 compared with LAI signal. Observed agricultural stages are (P1) wet sowings, (P2) emergence/seedling for groundnut, (P3) emergence/seedling to blooming for groundnut, blooming for the first sowing of millet and ear emergence stage for sorghum, (P4) pod formation for groundnut, blooming/ear emergence for millet and seedling to harvest stage for maize.

Dakar meteorological station. For each year of the studied period, the LAI time series were extracted within a 25 km radius around Dakar rain gauge station and averaged on the 4 soil classes and the corresponding vegetation classes (Fig. 5). Annual cumulative rainfall is also reported in Fig. 5. The four soils encountered in this region are raw mineral, hydromorphic, halomorphic and tropical ferruginous soils. Except for raw mineral soils covered by evergreen forests (GLC200), soil types are characterized by mixed vegetation comprising both natural vegetation (GLC110, GLC130 and GLC150 classes) and croplands (GLC14, GLC20 and GLC30, regrouped in the "crops" class in Fig. 5). The main results are as follows:

i. LAI signals were revealed to be strongly related to soil type. Except for the year 2006, crops developed on ferruginous tropical soils, are indeed characterized by a higher LAI signal (averaged LAI maximum of $1.10 \pm 0.19\ m^2\ m^{-2}$, period 2000–2008) than those developed on halomorphic ($0.68 \pm 0.06\ m^2\ m^{-2}$) and hydromorphic soils ($0.77 \pm 0.10\ m^2\ m^{-2}$). Vegetation density also has to be considered according to soil types: similar LAI signals for natural shrub (averaged maximum of 0.67 ± 0.06) are observed for the GLC110 (surface density ranged between 50 and 70%, halomorphic soil) and GLC130 classes (surface density $> 15\%$, hydromorphic soil). Similarly, LAI signals of the GLC150 class (surface density $< 15\%$, hydromorphic soil) are flattened.

ii. The link between MAP and LAI signals is not always *a priori* straightforward in Fig. 5. For example, the rainy year 2008 (MAP of 596.2 mm, Table 1) is correlated to a lower vegetation dynamics than the one observed in 2001 (MAP of 232.2 mm, Table 1). Moreover, if for some years the SOS and

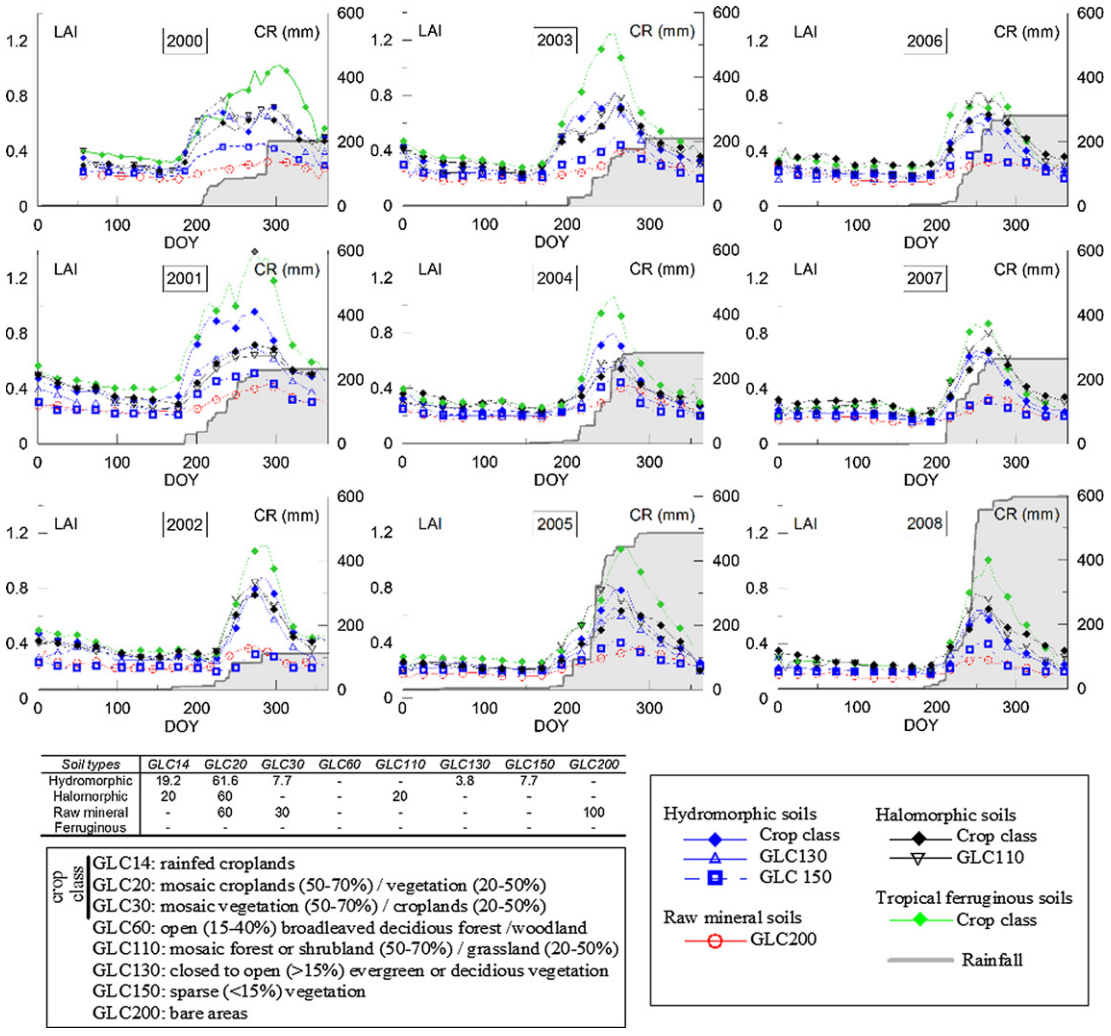

Fig. 5. Comparison of MODIS LAI and cumulative rainfall (CR) around Dakar for different types of soils and vegetation. The associated table expresses the different soil type fraction for each class of vegetation.

first rain events are synchronous (for years 2001, 2005, 2006, Fig. 5), rain interruptions occurring at the beginning of the rainy season may delay the emergence phase of the vegetation (such as for 2002 and 2004). It should also be pointed out that LAI onsets for the year 2003 are earlier than the onset of the rainy season. This singular observation could be attributed to the high spatial variability of precipitation (Ali et al., 2003) or, as it was reported by Hiernaux et al. (2009), in the Gourma site (Mali), could be explained by the presence of particular perennial herbs characterized by seasonal growth sometimes starting before the first rainfall event. Woody plant species observed by Tschakert and Tappan (2004) in the Old Peanut Basin such as *Adansonia digitata* (deciduous species) sprout indeed their leaves in the late dry season, which is partly explained by an access to water stored in the deeper ground layers or in the plant themselves, increasing therefore, their competitive ability against the evergreen and semi-evergreen species (De Bie et al., 1998).

In this study at 1 km^2 resolution, strong links between geomorphological features, soil moisture, and vegetation amount are highlighted through the analysis of MODIS LAI cycles. This interpretation supports work performed in other West African regions (Hiernaux et al., 2009; Kumar et al., 2002; Mougin et al., 2009) which have demonstrated that, in addition to rainfall variability, the annual productivity of herbaceous vegetation is controlled by the water run-on/run-off balance driven by soil types. Vegetation productivity on rocky soils or shallow soils is systematically low due to significant runoff. Herbs growing on clay soils (low permeability soils) in depressions, and experiencing flooding events during the rainy season, are characterized by a high variability, essentially depending on the success or failure of seed germination. Moreover, the low natural vegetation densities observed for raw mineral soils could also be explained by their high erodible properties and low fertility (Mougin et al., 2009). Additionally, it has been demonstrated in this study that the SOS and growth trends of crops developed on halomorphic soils are also slightly delayed compared with those developed on ferruginous tropical soils (Fig. 5). Hydromorphic soils (which can experience temporal changes in salinity due to groundwater pumping activities) and halomorphic soils are subject to human-induced salinization in the study area. These short delays are probably caused by high salt concentration in soils. Ramoliya and Pandey (2003) and Ramoliya et al. (2004) indeed observed minor delays in germination and growth of seedlings in saline environments.

5.2. Temporal and spatial vegetation seasonality at regional level

5.2.1. Spatial variation of phenological metrics

Maps of SOS, EOS and GSL (median values calculated over the period 2000–2008) are shown in Fig. 6. The SOS and EOS median values range from DOY 169-225 and DOY 284-347, respectively. Contrary to what was expected, the median SOS does not always follow the latitudinal rainfall gradient: localized areas, such as those observed west of Guéoul and Kébemer or, southwards, between Mékhé and Mboro and near Dakar, are characterized by early SOS (DOY 169-197, June 18th-July 16th). In the north of the study area, phenological events (late SOS and early EOS) appear to correlate well with Monsoon variability while temporal shifts in SOS and EOS are locally observed near the Thiès plateau and within the Lompoul-Kéllé-Kébemer area. The spatial variations of median EOS correlate with the latitudinal rain front, which progressively moves southwards at the end of the Monsoon season. The median EOS time lags are indeed estimated at about DOY 284-300 and DOY 314-347 in the northern and southern parts of the study area, respectively. The median GSL respectively varies between 74 days at Saint-Louis and 130 days at Dakar. At inter-annual and regional scales, it seems that the predominant factors controlling the GSL are both the duration of the rainy season (RS) and the MAP, which both tend to increase from the North to the South (Table 1). This result supports the work of Zhang et al. (2005), which highlights a north-south gradient in the SOS and EOS timings in Sahelian regions, with a respective average rate of 0.12 day/km and 0.05 day/km for the period 2000–2003. In north-western Senegal, and for the period 2000–2008, green-up onset and offset average rates are estimated in this work to 0.05 and 0.03 day/km, respectively.

5.2.2. Spatial variations of vegetation dynamics, relation with soil types

The influence of soil type on the LAI signal has been analysed through the MCV_LAI indicator. Fig. 7 presents the MCV_LAI calculated over the whole studied area at MODIS pixel scale. As shown on the map, it ranges between 7 and 71% with different signatures for raw mineral soils and ferruginous tropical soils. Raw mineral soils developed on live- and semi-fixed dunes are correlated to low MCV_LAI values, ranging between 7 and 37%. MCV_LAI values for ferruginous tropical soils range between 32 and 71%. A clear signature also appears south of Tivaouane between ferruginous tropical soils developed on marno-calcareous formations (MCV_LAI of 50–71%) and those developed on eolian formations (MCV_LAI of 38–49%). In addition, low spatial variations of MCV_LAI within a same type of soil (ferruginous tropical soils) are discernible. These could indicate changes in land-use practices and management and their consequences on vegetation density and soil fertility. Finally, landscapes located north of Louga and the area bounded by the cities of Mékhé, Mboro, Tiba Ndiaye and Tivaouane are defined by relatively low MCV_LAI values (32–45%).

5.3. Correlations between precipitation distribution and LAI seasonality

The correlations between precipitation and vegetation phenology metrics were analysed for the different vegetation types encountered around the four rain gauge stations (with radii defined in section 4.2).

5.3.1. Links between rainfall and LAI dynamics

The correlations between the rainfall parameters (MAP, *K* and *F*, see section 3.2) and the annual variation coefficient of LAI (CV_LAI) calculated for each year between 2000 and 2008, have been analysed. The objectives are to understand the role of the inter- and

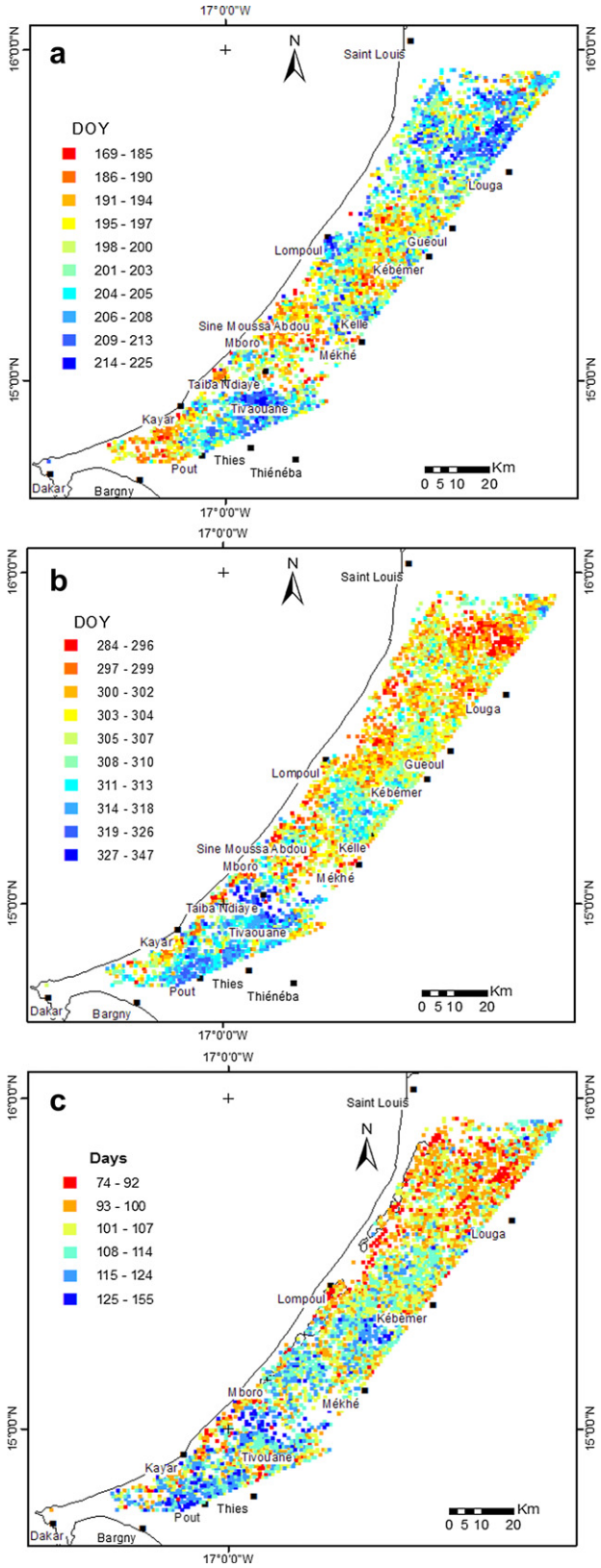

Fig. 6. Maps of median (a) SOS, (b) EOS and, (c) GSL for the period 2000–2008.

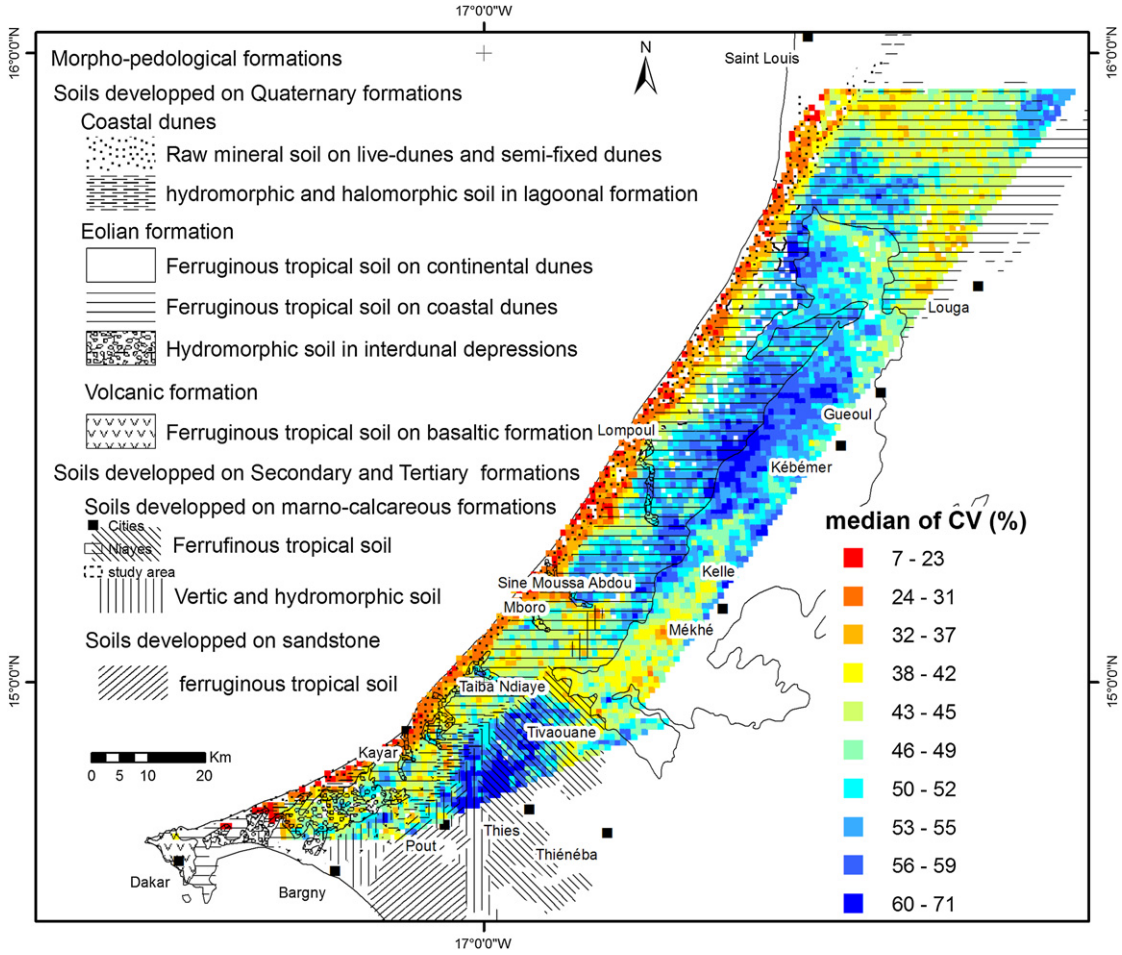

Fig. 7. Map of median CV of LAI (MCV_LAI) for the period 2000–2008.

intra-annual rainfall variability on the vegetation dynamics according to the different vegetation types.

Correlation coefficients (R-values) between CV_LAI and MAP, significant levels (P-values) and slopes (d) of linear regressions for different GLC classes are reported in Table 2. High P-values obtained for GLC130 and GLC150 classes do not allow the data to be interpreted. Significant correlations are observed between MAP and CV_LAI (R: 0.64, Table 2), which range from 0.58 to 0.70 for crops and from 0.62 to 0.72 for natural vegetation. Slopes for crops and GLC110 classes are similar, revealing the same vegetation response to MAP. The slope for the GLC140 class is twice as steep and thus demonstrates the larger sensitivity of natural herbs to rainfall.

Moreover, moderate but significant CV_LAI and K (R: 0.51, Table 2) relationships are highlighted. This correlation is particularly strong for grassland (GLC140) and sparse vegetation (GLC150) classes. This demonstrates that the dynamics of natural herbs is highly dependent on the rainfall frequency within the rainy season. This observation is in agreement with ground surveys carried out in Niger (Boulain et al., 2009), which showed the particularly unfavourable effects of dry spells during the rainy season on vegetation (millet and fallow) biomass development.

The last rainfall parameter used, F (see section 3.2), takes into account both the MAP and the precipitation distribution during the Monsoon season. The correlation between CV_LAI and F is noticeably higher (compared to the CV_LAI – MAP correlation) and is equal to 0.70 on the whole region (Table 2). In addition, different vegetation responses, or sensitivities, to the rainfall distribution can be identified: similar correlation values for crops using CV_LAI-

Table 2
Correlation coefficients between CV of LAI and MAP ($R_{MAP/CV}$), K parameter ($R_{K/CV}$) and F parameter ($R_{F/CV}$) and corresponding P-values. Slopes of linear fits (labelled d) are also reported.

	GLC14	GLC20	GLC30	GLC110	GLC130	GLC140	GLC150	GLC
$R_{MAP/CV}$	0.67	0.70	0.58	0.72	0.06	0.62	0.29	0.64
P-value	$<10^{-3}$	$<10^{-3}$	$<10^{-3}$	$<10^{-2}$	0.905	0.077	0.232	$\ll10^{-3}$
d	0.050	0.063	0.043	0.057	0.004	0.081	0.023	
$R_{K/CV}$	0.48	0.54	0.42	0.39	0.19	0.56	0.56	0.51
P-value	0.015	0.005	0.014	0.145	0.683	0.115	0.016	$\ll10^{-3}$
d	70.4	93.5	58.3	65.6	30.6	52.6	66.9	
$R_{F/CV}$	0.65	0.70	0.58	0.67	0.13	0.77	0.41	0.70
P-value	$<10^{-3}$	$<10^{-3}$	$<10^{-3}$	$<10^{-2}$	0.784	0.015	0.093	$\ll10^{-3}$
d	0.108	0.138	0.096	0.121	0.019	0.218	0.085	

MAP or CV_LAI -F couples are observed when these correlations are much improved for natural herbs (GLC140) using the parameter *F*. The similar correlation values for crops observed in the study area, using MAP or *F* indicators (Fig. 7), could be partially explained by local human-induced practices, which aim at controlling and improving cereal productivity, and at reducing the negative influence of the erratic rainfall. For example, for ensuring a good food crop production, if plant stress occurs after a rainfall interruption at the beginning of the rainy season, a second sowing is performed. Land-use practices may maintain productivity crops up to certain rainfall conditions: for the driest years, interruption in rain during the greening-up period is also responsible for a succession of sowings and aborted germination, which sometimes leads to the exhaustion of seed stock and low vegetation productivity (Boulain et al., 2009; Sultan et al., 2005).

5.3.2. Predicting the SOS

Numerous rainfall indicators have been used for monitoring vegetation. Those frequently used are relative and absolute cumulative rainfall thresholds (Zhang et al., 2005), percentage of MAP (White et al., 1997) and soil moisture index (Lyamchai et al., 1997). In this study, we follow the Zhang et al.'s (2005) methodology: cumulative rainfall thresholds, ranging from 5 to 100 mm have been defined and, for each threshold, we calculated the rainfall threshold date (RTD, in DOY). We compared (for each year of the studied period) the SOS to the dates (RTD) at which those thresholds are reached (Table 3). Here, the beginning of the rainy season is considered as the first rain event from DOY 150 (Heug rains are not taken into account). *R*-values between SOS and RTDs (Table 3) indicate the optimal rainfall thresholds for the development of the different vegetation classes.

Several vegetation behaviours emerge:

i. Significant SOS-RTD correlations for rain-fed crops (GLC14, GLC20 and GLC30) may be seen when the cumulated rainfall reaches 20 mm.
ii. Moderate correlation for the GLC110 class is observed for a 5 mm threshold (*R*: 0.41), which tends to increase with rainfall amounts up to a threshold of 40 mm (*R*: 0.86). Such a wide window of significant responses probably results from the specificities of this class which is composed of both grassland and mixed shrub/forest vegetation.
iii. High *R*-values (*R*: 0.68) characterizing shrub land cover (GLC130) appear for a 40 mm threshold while significant *R*-values are observed for open to closed grassland (GLC140 and GLC143) from the start of the rainy season.
iv. Significant SOS-RTD correlations are observed for a 10–20 mm threshold for sparse vegetation (GLC150).

Table 3
Correlation coefficients between dates of RTDs and SOS for different GLC classes. BR is the start of the rainy season.

	Glc14	Glc20	Glc30	Glc110	Glc130	Glc140	Glc143	Glc150
BR	−0.36	−0.29	−0.08	−0.19	0.15	0.21	0.45	0.09
5	−0.07	−0.03	−0.14	0.41	0.25	−0.09	0.26	0.35
10	−0.01	0.01	0.26	0.52	0.26	−0.11	0.31	0.45
20	0.43	0.43	0.49	0.66	0.18	0.05	0.36	0.23
30	0.46	0.45	0.48	0.79	0.39	0.10	0.40	−0.01
40	0.35	0.34	0.42	0.86	0.68	0.09	0.44	−0.14
50	0.41	0.40	0.35	0.81	0.58	0.20	0.31	−0.25
60	0.48	0.47	0.32	0.79	0.47	0.16	0.23	−0.12
70	0.43	0.43	0.29	0.78	0.44	0.19	0.24	−0.16
80	0.46	0.48	0.30	0.84	0.48	0.52	0.32	−0.05
90	0.28	0.25	0.23	0.84	0.47	0.54	0.38	−0.34
100	0.22	0.25	0.20	0.55	0.29	0.51	0.39	−0.09

The correlations between RTDs and SOS from LAI data turn out to be helpful for monitoring vegetation biomass in Sahel. Coupled with weather forecasting models, such indices could be helpful for predicting vegetation growth.

6. Conclusion

The agricultural eco-regions of the "Peanut basin" and "Long Coast", located in northwestern Senegal, are subject to erratic rainfall and to an extension of human land-use practices which lead to vegetation biomass decrease. One means of assessing recent changes (period 2000–2008) in vegetation productivity and seasonality and understanding these changes at a regional scale is to couple MODIS LAI time series with daily rainfall and land cover information. Although the datasets used in this study (soil and land cover maps, precipitation data and satellite products), may present various sources of uncertainties, the analysis of all these data at regional scale permitted us to extract strong patterns and our main results may be summarized as follows:

i) The analysis of MODIS LAI time series at pixel scale does not allow the different types of vegetation to be described nor the land cover changes to be evaluated. However, the analysis performed near the station of Thiès indicates that LAI signals strongly follow the actual phenological stages in cropland regions, the latter being itself strongly related to precipitation trends.
ii) Dynamics of vegetation are strongly correlated to soil types and inherent differences in fertility, and thus agricultural practices: vegetation developed on ferruginous tropical soils corresponds to high LAI signal seasonal amplitudes, compared to raw mineral soils, hydromorphic and halomorphic soils.
iii) Observations made at the 1 km^2 scale are validated at regional scale through the analysis of MCV_LAI map. Different MCV_LAI ranges were identified according to soil types. A main difference in MCV_LAI values is revealed between ferruginous tropical soils (high MCV_LAI) and raw mineral soils (low MCV_LAI), discernible by a clear longitudinal border between live-dunes and landscape located eastwards. Moreover, local anomalies of the MCV_LAI within a same type of soil (ferruginous tropical soils) probably indicate changes in land-use practices and management and their consequences on vegetation density and soil fertility. Historical and current land cover management (Affholder, 1995; Hiernaux et al., 2009; Tschakert, 2007; Tschakert and Tappan, 2004; Tottrup and Rasmussen, 2004) as well as socio-economic (Brown and de Beurs, 2008) knowledge needs to be superimposed onto natural factors to explain local moderate LAI signal differences within a same type of soil. The derivation of phenological information from LAI time series, through the calculation of the annual CV and the estimation of phenological metrics (SOS and EOS dates, GSL), helps to understand the vegetation intra-seasonal and inter-annual variations. More particularly, at inter-annual and regional scales, the map of median GSL seems to depend on both the length of the rainy season and MAP, and tends to follow the latitudinal negative gradient.
iv) Both the MAP and the distribution frequency of rainy events (K) during the Monsoon period control the vegetation dynamics (annual CV of LAI). Moreover, the introduction of the parameter *F*, taking into account both MAP and *K*, reinforce the correlation between vegetation productivity and climatic trends, the latter being particularly enhanced for natural grasslands. These two climatic indicators could be applied to other semi-arid environments for predicting

changes in vegetation growth and productivity using climatic scenarios.

v) Combining RTDs with SOS dates are pertinent for monitoring the green-leaf emergence for the different types of Sahelian vegetation.

This study has been focused on the northwest part of Senegal to benefit from the collaboration network within the SAHELP (Sahara and SAHEL vulnerability: lessons from the Past) project. A similar approach will be soon applied to the Ferlo region in the framework of the AMMA (African Monsoon Multidisciplinary Analyses) program (Cissé et al., personal communication) using satellite precipitation product as those provided by the Tropical Rainfall Measuring Mission (TRMM) satellite. The use of such spatialized dataset should allow to better understand and quantify the strong relationships between vegetation seasonal activity and rainfall in sahelian environments.

Acknowledgements

This study was performed with financial support of GIS (Climat-Environnement-Société) and SAHELP projects. We are grateful to the Senegalese "Direction Nationale de la Météorologie" for the facilities that have contributed to the achievement of this work. The authors acknowledge GES DAAC MODIS Data Support Team for making MODIS data available to the user community, as well as our colleague Seyni Salack for his helpful suggestions.

References

Affholder, F., 1995. Effect of organic matter input on the water balance and yield of millet under tropical dryland condition. Field Crops Research 41, 109–121.

Ali, A., Lebel, T., Amani, A., 2003. Invariance in the spatial structure of Sahelian rain fields at climatological scales. Journal of Hydrometeorology 4 (6), 996–1011.

Bicheron, P., Leroy, M., Brockmann, C., Krämer, U., Miras, B., Huc, M., Nino, F., Defourny, P., Vancutsem, Ch., Arino, O., Ranéra, F., Petit, D., Amberg, V., Berthelot, B., Gross, D., 2006. GLOBCOVER: a 300 m global land cover product for 2005 using ENVISAT/MERIS time series. In: International Symposium on Recent Advances in Quantitative Remote Sensing, Torrent, Spain.

Boulain, N., Cappelaere, B., Ramier, D., Issoufou, H.B.A., Halilou, O., Seghieri, J., Guillemin, F., Oï, M., Gignoux, J., Timouk, F., 2009. Towards an understanding of coupled physical and biological processes in the cultivated Sahel ± 2. Vegetation and carbon dynamics. Journal of Hydrology 375, 190–203.

Brown, M.E., de Beurs, K.M., 2008. Evaluation of multi-sensor semi-arid crop season parameters based on NDVI and rainfall. Remote Sensing of Environment 112, 2261–2271.

Cuenca, R.H., Brouwer, J., Chanzy, A., Droogers, P., Galle, S., Gaze, S.R., Sicot, M., Stricker, H., Angulo-Jaramillo, R., Boyle, S.A., Bromley, J., Chebhouni, A.G., Cooper, J.D., Dixon, A.J., Fies, J.-C., Gandah, M., Gaudu, J.-C., Laguerre, L., Lecocq, J., Soet, M., Steward, H.J., Vandervaere, J.P., Vauclin, M., 1997. Soil measurements during HAPEX-Sahel Intensive observation period. Journal of Hydrology 188–189, 224–266.

De Bie, S., Ketner, P., Paasse, M., Geerling, C., 1998. Woody plant phenology in the West Africa savanna. Journal of Biogeography 25, 883–900.

Diouf, A., Lambin, E.F., 2001. Monitoring land-cover changes in semi-arid regions: remote sensing data and field observations in the Ferlo, Senegal. Journal of Arid Environments 48, 129–148.

Doraiswamy, P.C., Sinclair, T.R., Hollinger, S., Akhmedov, B., Stern, A., Prueger, J., 2005. Application of MODIS derived parameters for regional crop yield assessment. Remote Sensing of Environment 97, 192–202.

Fensholt, R., Sandholt, I., Rasmussen, M.S., 2004. Evaluation of MODIS LAI, fAPAR and the relation between fAPAR and NDVI in a semi-arid environment using in situ measurements. Remote Sensing of Environment 91, 490–507.

Fisher, J.I., Mustard, J.F., 2007. Cross-scalar satellite phenology from ground, Landsat, and MODIS data. Remote Sensing of Environment 109, 261–273.

Gaze, S.R., Brouwer, J., Simmonds, L.P., Bromley, J., 1998. Dry season water use patterns under *Guiera senegalensis* L. shrubs in a tropical savanna. Journal of Arid Environments 40, 53–67.

Gonzalez, P., 1997. Dynamics of Biodiversity and human carrying capacity in the Senegal Sahel, Ph.D. Dissertation, University of California, Berkeley.

Gonzalez, P., 2001. Desertification and a shift of forest species in the West African Sahel. Climate Research 17, 217–228.

Hiernaux, P., Mougin, E., Diarra, L., Soumaguel, N., Lavenu, F., Tracol, Y., Diawara, M., 2009. Sahelian rangeland response to changes in rainfall over two decades in the Gourma region, Mali. Journal of Hydrology 375, 114–127.

Jiang, B., Liang, S., Wang, J., Xiao, Z., 2010. Modeling MODIS LAI time series using three statistical methods. Remote Sensing of Environment 114, 1432–1444.

Kang, S., Running, S.W., Lim, J.-H., Zhao, M., Park, C.-R., Loehman, R., 2003. A regional phenology model for detecting onset of greenness in temperate mixed forests, Korea: an application of MODIS leaf area index. Remote Sensing of Environment 86, 232–242.

Kaptue Tchuente, A.T., Roujean, J.-L., Faroux, S., 2010. ECOCLIMAP-II: an ecosystem classification and land surface parameters database of Western Africa at 1 km resolution for the African Monsoon Multidisciplinary Analysis (AMMA) project. Remote Sensing of Environment 114, 961–976.

Knyazikhin, Y., Glassy, J., Privette, J. L., Tian, P., Lotsch, A., Zhang, Y., Wang, Y., Morisette, J. T., Votava, P., Myneni, R. B., Nemani, R. R., Running, S. W., 1999. MODIS Leaf Area Index (LAI) and fraction of photosynthetically active radiation absorbed by vegetation (fPAR). Product (MOD15) Algorithm Theoretical Basis Document.

Kramer, K., Leinonen, I., Loustau, D., 2000. The importance of phenology for the evaluation of impact of climate change on growth of boreal, temperate and mediterranean forest ecosystems: an overview. International Journal of Biometeorology 44, 67–75.

Kumar, L., Rietkerk, M., van Langevelde, F., van de Koppel, J., van Andel, J., Hearne, J., de Ridder, N., Stroosnijder, L., Skidmore, A.K., Prins, H.H.T., 2002. Relationship between vegetation growth rates at the onset of the wet season and soil type in the Sahel of Burkina Faso: implications for resource utilisation at large scales. Ecological Modelling 149, 143–152.

Lebel, T., Ali, A., 2009. Recent trends in the Central and Western Sahel rainfall regime (1990–2007). Journal of Hydrology 375, 52–64.

Le Borgne, A., 1979. Un exemple d'invasion polaire sur la région mauritano sénégalaise. Annals of Géography 489, 521–548.

Lyamchai, C.J., Gillespie, T.J., Brown, D.M., 1997. Estimating maize yield in northern Tanzania by adapting SIMCOY, a temperate-zone simulation model. Agricultural and Forest Meteorology 85, 75–86.

Malhado, A.C.M., Malhi, Y., Whittaker, R.J., 2009. Spatial trends in leaf size of Amazonian rainforest trees. Biogeosciences 6, 1565–1676.

Mougin, E., Hiernaux, P., Kergoat, L., Grippa, M., de Rosnay, P., Timouk, F., Le Dantec, V., Demarez, V., Lavenu, F., Arjounin, M., Lebel, T., Soumaguel, N., Ceschia, E., Mougenot, B., Baup, F., Frappart, F., Frison, P.L., Gardelle, J., Gruhier, C., Jarlan, L., Mangiarotti, S., Sanou, B., Tracol, Y., Guichard, F., Trichon, V., Diarra, L., Soumaré, A., Koité, M., Dembélé, F., Lloyd, C., Hanan, N.P., Damesin, C., Delon, C., Serça, D., Galy-Lacaux, C., Seghieri, J., Becerra, S., Dia, H., Gangneron, F., Mazzega, P., 2009. The AMMA-CATCH Gourma observatory site in Mali: relating climatic variations to changes in vegetation, surface hydrology, fluxes and natural resources. Journal of Hydrology 375, 14–33.

Myneni, R.B., Nemani, R.R., Running, S.W., 1997. Estimation of global leaf area index and absorbed PAR using radiative transfer model. IEEE Transactions on Geo-Science and Remote Sensing 35, 1380–1393.

Myneni, R.B., Knyazikhin, Y., Privette, J.L., Glassy, J., Tian, Y., Wang, Y., Hoffman, S., Song, X., Zhang, Y., Smith, G.R., Lotsch, A., Friedl, M., Morisette, J.T., Votava, P., Nemani, R.R., Running, S.W., 2002. Global products of vegetation leaf area and fraction absorbed PAR from year one of MODIS data. Remote Sensing of Environment 83, 214–231.

Nicholson, S., 2000. Land surface processes and Sahel climate. Reviews of Geophysics 38, 117–139.

Nicholson, S., 2005. On the question of the "recovery" of the rains in the West African Sahel. Journal of Arid Environments 63, 615–641.

Olsson, L., Eklundh, L., Ardö, J., 2005. A recent greening of the Sahel—trends, patterns and potential causes. Journal of Arid Environments 63, 556–566.

Omotosho, J.B., 1992. Long-range prediction of the onset and end of the rainy season in the west African Sahel. International Journal of Climatology 12 (4), 369–382.

Peñuelas, J., Filella, I., Zhang, X.Y., Llorens, L., Ogaya, R., Lloret, F., Comas, P., Estiarte, M., Terradas, J., 2004. Complex spatiotemporal phonological shifts as a response to rainfall changes. New Phytology 161 (3), 837–846.

Privette, J.L., Myneni, R.B., Knyazikhin, Y., Mukelabai, M., Roberts, G., Tian, Y., Wang, Y., Leblanc, S.G., 2002. Early spatial and temporal validation of MODIS LAI product in the Southern Africa Kalahari. Remote Sensing of Environment 83, 232–243.

Proud, R.S., Rasmussen, L.V., 2011. The influence of seasonal rainfall upon Sahel vegetation. Remote Sensing Letters 2 (3), 241–249.

Ramoliya, P.J., Pandey, A.N., 2003. Effect of salinization of soil on emergence, growth and survival of seedlings of Cordia rothii. Forest Ecology and Management 176, 185–194.

Ramoliya, P.J., Patel, H.M., Pandey, A.N., 2004. Effect of salinization of soil on growth and macro-and micro-nutrient accumulation in seedlings of Salvadora persica (Salvadoraceae). Forest Ecology and Management 202, 181–193.

Schwartz, M.D., 1998. Green-wave phenology. Nature 394, 839–840.

Stancioff, A., Staljanssens, M, Tappan, G., 1986. Cartographie et Teledetection des Ressources de la Republique du Senegal: Etude de la Geologie, de l'Hydrologie, des Sols, de la Vegetation et des Potentiels d'Utilisation des Sols. SDSU-RSI-86-01.

Sultan, B., Baron, C., Dingkuhn, M., Sarr, B., Janicot, S., 2005. Agricultural impacts of large-scale variability of the West African monsoon. Agricultural and Forest Meteorology 128, 93–110.

Tappan, G., Hadj, A., Wood, E., Lietzow, R., 2000. Use of argon, corona, and Landsat imagery to assess 30 years of land resource changes in west-central Senegal. Photogrammetric Engineering and Remote Sensing 66 (6), 727–735.

Tappan, G.G., Sall, M., Wood, E.C., Cushing, M., 2004. Ecoregions and land cover trends in Senegal. Journal of Arid Environments 59, 427–462.

Tottrup, C., Rasmussen, M.S., 2004. Mapping long-term changes in savannah crop productivity in Senegal through trend analysis of time series of remote sensing data. Agriculture Ecosystems and Environment 103, 545–560.
Tschakert, P., Tappan, G., 2004. The social context of carbon sequestration: considerations from a multi-scale environmental history of the Old Peanut Basin of Senegal. Journal of Arid Environments 59, 535–564.
Tschakert, P., 2007. Views from the vulnerable: understanding climatic and other stressors in the Sahel. Global Environmental Change 17, 381–396.
Tucker, C.J., Townshend, J.R., Goff, T.E., 1985. African land-cover classification using satellite data. Science 227 (4685), 369–375.
UNCCD, 1994. Elaboration of an International Convention to Combat Desertification in Countries Experiencing Serious Drought and/or Desertification, Partricularly in Africa. United Nations General Assembly, 93rd Plenary Meeting, New York.
White, M.A., Thornton, P.E., Running, S.W., 1997. A continental phenology model for monitoring vegetation responses to inter-annual climatic variability. Global Biogeochemical Cycles 11, 217–234.
White, M.A., Nemani, R.R., Thornton, P.E., Running, S.W., 2002. Satellite evidence of phenological differences between urbanized and rural areas of the eastern United States deciduous broadleaf forest. Ecosystems 5, 260–277.
Zhang, X., Friedl, M.A., Schaaf, C.B., Strahler, A.H., Hodges, J.C.F., Gao, F., Reed, B.C., Huete, A., 2003. Monitoring vegetation phenology using MODIS. Remote Sensing of Environment 84, 471–475.
Zhang, X., Friedl, M.A., Schaaf, C.B., Strahler, A.H., Liu, Z., 2005. Monitoring the response of vegetation phenology to precipitation in Africa by coupling MODIS and TRMM instruments. Journal of Geophysical Research 110, D12103. doi:10.1029/2004JD005263.